Crowd Simulation: Improving Pedestrians' Dynamics by the Application of Lattice-Gas Concepts to the Social Force Model

Priscila Saboia and Siome Goldenstein
Institute of Computing
University of Campinas, Unicamp
Campinas (SP), Brazil
{psaboia, siome}@ic.unicamp.br

***Abstract*—The social force (SF) model has been successfully applied to the simulation of flows of pedestrians. Nevertheless, in some scenarios with low density, experiments show that the simulated individuals do not behave as expected, working as irrational particles rather than smart people. For example, by the means of the cited model, it is common to see many simulated individuals going several times straightly against columns, before finding a way to deviate and safely exit the room. Aiming to deal with such problems, this article proposes a way to provide the simulated pedestrians the ability of changing the direction of their displacement at reasonable times, in order to bypass eventually blocked or crowded near areas. To do so, it applies concepts from the lattice-gas model to the SF model. Experiments were driven in order to evaluate the proposed model. As results, it maintained the ability of the SF model to reproduce phenomena like the formation of arcs in evacuated one-door rooms. Focusing on the scenario with a column-blocked one-door room, the simulated pedestrians presented softer and more coherent trajectories, when compared to the pure SF model solution.**

***Keywords*-crowd simulation; social force model; lattice-gas model;**

I. Introduction

Crowds can be seen as a large group of individuals put together in the same physical environment, sharing a common goal and acting differently from how they would act if they were alone. Understanding the movement of crowds is very important for planning and improving public places, not only in order to facilitate and expedite the movement of citizens, but also to guarantee their safety, especially in conditions of imminent danger, where it can be necessary the evacuation of such sites.

Dynamic aspects of evacuation processes have been characterized through modeling, due to the absence of data from real evacuations. Several computer models have been proposed in this direction. Among these models, there is the social force one, proposed by Helbing and Molnar [1], in which the motion of each pedestrian is subjected to physical and psychological forces. This model describes successfully some phenomena, such as arching and the "Faster-is-slower" one.

Nevertheless, this model may produce counterintuitive results when applied to the movement of a rare group of pedestrians, i.e. in big places where the density of people is low or moderate. Thus, in these scenarios, the trajectories of pedestrians are similar to the trajectories of particles rather than similar to the trajectories of real people.

Contributions: We present a modification of the SF model in order to overcome the difficulties cited above. In particular, we redesigned one of the forces of the SF model (the so-called force of desire), in order to allow pedestrians to change voluntarily their desired directions of movement, based on their perceptions of other pedestrians and obstacles in the neighborhood. So, we mapped the space around each pedestrian as an adaptive grid (as in [2]) as a manner to obtain spatial information about the neighborhood and to choose the direction of the force of desire used in the SF model. In our experiments, we show that the modified model improves the trajectories of the pedestrians, while maintaining its ability to reproduce the "Faster-is-slower" effect and the arching underlying the clogging effects.

A. Related work

We can roughly classify the approaches used for crowd simulation into two categories: discrete-space and continuous-space models.

Discrete-space models are usually based on cellular automata models, in which pedestrians are located at nodes of a grid and their coordinates are updated at discrete time intervals. Example models of this approach are described in Varas et al. [3] and Perez et al. [4]. There are also models in this category based on lattice-gas concepts, that is a special case of cellular automata. In these models, the pedestrians' movement occurs as probabilistic and statistic functions, as one can see in the work proposed by Muramatsu et al. [5]; Tajima and Nagatani [6]; and Guo and Huang [2].

In the continuous-space models, the pedestrians may move continually in a 2-D surface. Within this approach, there are the fluid-dynamic models and the social force ones. Fluid-dynamic models describe the dynamic of the density and velocity of the crowd by the means of partial differential equations. Examples of this approach can be found in the work of Hughes [7], Huang et al. [8] and Treuille et al. [9]. Finally, the social force models introduced by Helbing and Molnar [1] describe the motion of each pedestrian as a result of physical

and psychological forces. Once in this paper we modified this last model, it is presented in more detail in the next section.

II. The Social Force Model

In this section, we describe the social force model (SF), proposed by Helbing and Molnar [1]. In this model, each pedestrian determines its motion taking into account three types of effects that rely on physical and psychological forces.

A. Effect of a pedestrian's desire

Each pedestrian i of mass m_i wants to reach a target position r_i^0. By doing so, a pedestrian has got a predefined speed v_i^0 (i.e. desired velocity) in a certain direction e_i. If $r_i(t)$ is the present position of a pedestrian i, at time t, its desired direction of motion $e_i(t)$ will be

$$e_i(t) = \frac{r_i^0 - r_i(t)}{|r_i^0 - r_i(t)|}, \tag{1}$$

to which the pedestrian tends to adapt its instantaneous velocity v_i within a certain time interval τ. Then, the effect of a pedestrian's desire can be described by the force

$$f_i^D(t) = m_i \frac{1}{\tau}(v_i^0 e_i(t) - v_i(t)). \tag{2}$$

B. Repulsive effect due to other pedestrians (or obstacles)

Pedestrians try to keep a certain distance from other entities j (i.e. other pedestrians or obstacles) by an interaction force

$$f_i^R = \sum_{j=1, j\neq i}^{N_p} \mathrm{A}\exp(\frac{-x_{ij}}{\mathrm{B}})n_{ij}, \tag{3}$$

where A represents the intensity of the repulsive force measured in Newtons, and B is a constant value which determines the range of the social interaction, measured in meters. $n_{ij} = (n_{ij}^1, n_{ij}^2)$ is the two-dimensional unit vector pointing from the pedestrian (or obstacle) j to the pedestrian i, and x_{ij} is the distance between a pedestrian i and a pedestrian (or an obstacle) j. It is important to notice that pedestrians are modeled geometrically as circles, whereas obstacles (i.e. walls, columns, doors, etc) are modeled as polygons. N_p represents the total number of pedestrians and obstacles in the model.

C. Granular interaction effects in panicking crowds

The authors assume two additional forces inspired by granular interactions which are essential to understand the particular effects in panicking crowds: a body force $k(-x_{ij})n_{ij}$, that prevents body compression, and a sliding friction force $\kappa(-x_{ij})\Delta v_{ji}^t t_{ij}$ that interferes in the relative tangential motion, if pedestrian i comes close to j. Here, $t_{ij} = (-n_{ij}^2, n_{ij}^1)$ means the tangential direction, and Δv_{ji}^t means the tangential velocity difference, while k and κ represent constants. Thus, we have

$$f_i^G = \sum_{j=1, j\neq i}^{N_p} K\Theta(-x_{ij})n_{ij} + \kappa\Theta(-x_{ij})\Delta v_{ji}^t t_{ij}, \tag{4}$$

where the function $\Theta(x)$ is zero if the pedestrians do not touch each other. Otherwise, it is equal to the argument x. In the case of interactions involving a pedestrian and objects, the effect of this force is described similarly.

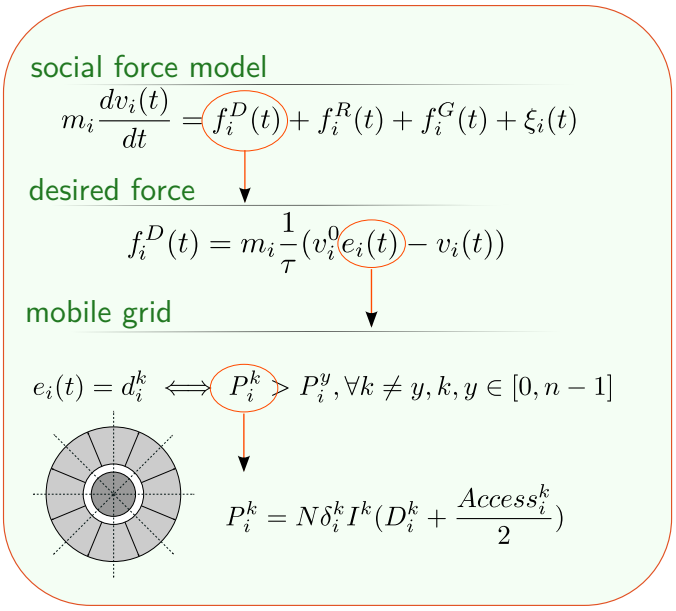

Fig. 1. Illustration of the proposed method.

D. Motion of a pedestrian

The change of velocity in time t is given by the acceleration equation:

$$m_i \frac{dv_i(t)}{dt} = f_i^D(t) + f_i^R(t) + f_i^G(t) + \xi_i(t), \tag{5}$$

where $\xi_i(t)$ represents a fluctuation term that stands for random behavioural variations arising from accidental or deliberate deviations from the optimal strategy of motion. Finally, the change of position $r_i(t)$ is given by the velocity $v_i(t) = dr_i(t)/dt$.

E. Our proposal

The SF model generates realistic phenomena such as arching around exits. However, in this model, the desired direction $e_i(t)$ of motion of a pedestrian i always points to the same target position r_i^0 even in the presence of obstacles (or other pedestrians) between its current position $r_i(t)$ and the target position. So, in some evacuation cases, the trajectories of pedestrians are similar to the trajectories of particles rather than to the trajectories of people. For example, it is common to see many simulated individuals going several times straightly against columns before finding a way to deviate and safely exit the room.

Thinking about this problem, we present a modification of the SF model, redesigning the force of desire (Equation 2) in order to permit pedestrians to change their desired direction ($e_i(t)$) of movement voluntarily, based on their perceptions of other pedestrians and obstacles in their neighborhood. So, the new desired direction is obtained by a mobile grid from the lattice-gas model [2]. The mobile grid divides the area around

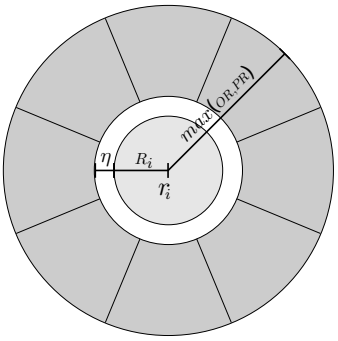

Fig. 2. Mobile grid partitioned into 8 directions around a pedestrian i.

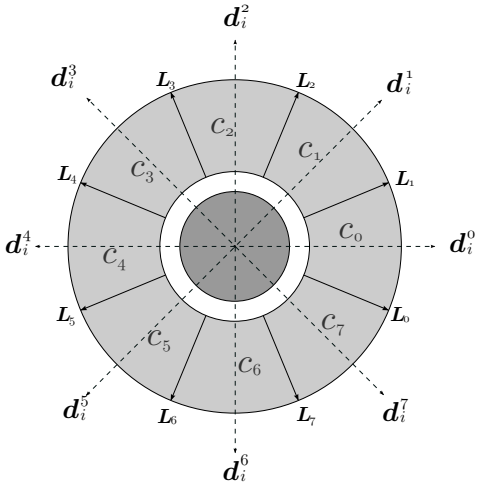

Fig. 3. Lattices and directions of a mobile grid.

a pedestrian into n directions, each one with an associated weight value. At each time t, the desired direction is the one with the greatest weight value. This modified model is illustrated in (Fig. 1).

III. The Modified SF Model

Our proposal aims to change the direction of the force of desire in the SF model, so that pedestrians can deliberately circumvent other pedestrians and obstacles. To do so, the direction is obtained by a mobile grid similar to that used in [2]. The mobile grid proposed in our work is specified below.

A. Mobile Grid

Just as in the SF model, each pedestrian i is represented by a circle of radius R_i. The mobile grid can be defined as an area formed by an annulus around a pedestrian i, evenly partitioned into n directions. It is conventional to name as lattice each one of the partitions, denoted by c_k, where $k \in \{0, n-1\}$. The annulus is formed by two concentric circles of center $r_i(t)$, where the inner radius of the circle is given by $R_i + \eta$, and the radius of the external circumference is given by the radius of the pedestrian's greatest neighborhood, i.e. $max(PR, OR)$, where PR represents the radius of the neighborhood of the

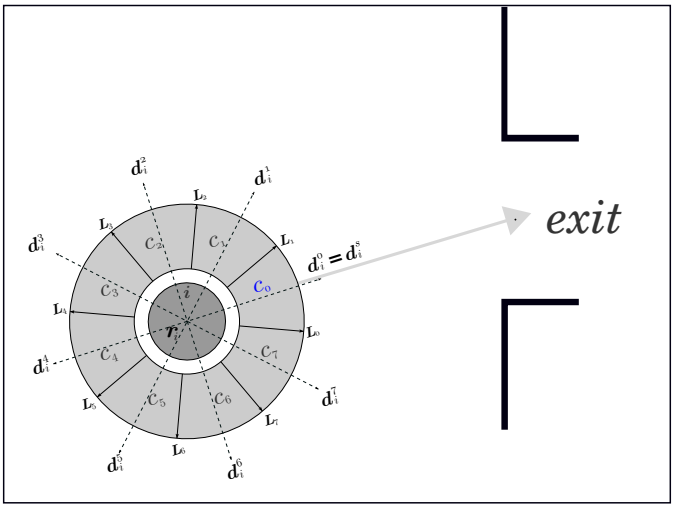

Fig. 4. Grid in the absence of obstacles in the direction of the vector d_i^s.

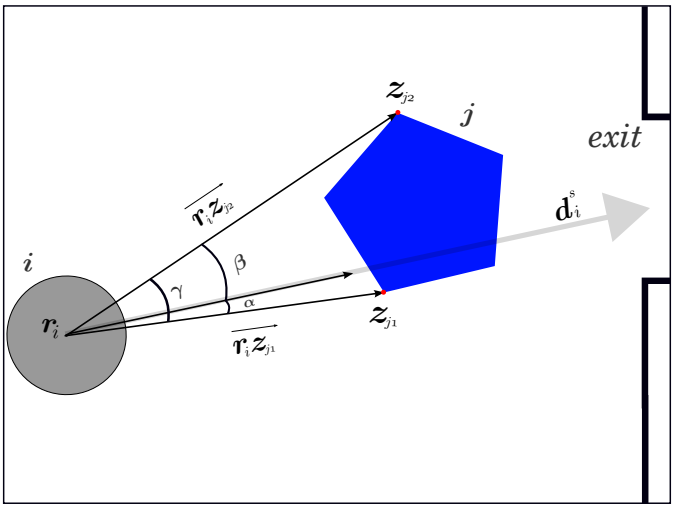

Fig. 5. Endpoints z_{j1} and z_{j2} of the object j.

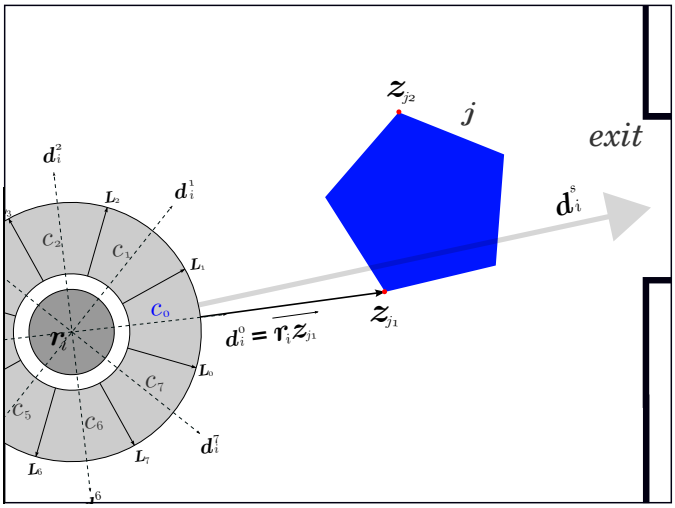

Fig. 6. Grid in the presence of an obstacle j in the direction of the vector d_i^s.

pedestrian i in relation to other pedestrians, and OR represents the radius of the neighborhood in relation to obstacles. The constant η represents the minimum distance at which a pedestrian desires to be from other pedestrians and obstacles. Fig. 2 shows a pedestrian's current position and an annulus around it.

The lattices are bounded by vectors in the sequence $L_0, L_1, ..., L_{n-1}$, as illustrated in Fig. 3. Each lattice c_k has an opening angle $\theta = 360/n$, a direction defined by the vector d_i^k, and two limiting unit vectors L_a and L_b, respectively put in a counterclockwise direction, with $a = (i \mod n)$ and $b = ((i+1) \mod n)$.

Moreover, lattices are arranged in the counterclockwise direction on the basis of the output vector d_i^s (obtained in the same way that e_i in Equation 1). In the absence of obstacles in the direction of the vector d_i^s, the grid is arranged so that the lattice c_0 has its representative vector $d_i^0 = d_i^s$, (Fig. 4). Otherwise, the direction of d_i^0 is obtained by taking into account the vector d_i^s and the endpoints of the object j (which in this case is an obstacle) in relation to the pedestrian i. Considering the points z_{j1} and z_{j2} as endpoints of the object j, they are obtained based on the angle subtended by j to $r_i(t)$, which is the center of the pedestrian i, as one can see in Fig. 5. Thus, once defined the endpoints and data vectors $r_i z_{j1}$ and $r_i z_{j2}$, the vector d_i^0 is equal to the vector among those which present the highest angle with the vector d_i^s (Fig. 6).

It is important not to lose sight that the grid is used in order to obtain the new desired direction of the velocity $e_i(t)$ used in Equation 2. For that, there is a weight distribution (P_i^k) between its lattices, indicating the likelihood of choosing each one. The direction of the chosen lattice will be the new desired direction of the velocity. The distribution of weights for lattices is explained in the next section.

B. Distribution of weights

For a pedestrian i, the distribution of weights for each lattice k is denoted by P_i^k and obtained as follows:

$$P_i^k = N\delta_i^k I^k (D_i^k + \frac{Access_i^k}{2}). \tag{6}$$

The term $Access_i^k$ represents the measure of accessibility of the lattice c_k to a pedestrian i. The higher the value of access, more accessible is the lattice

$$Access_i^k = \min_{j \in \Omega_i} (S_{ij}^k), \tag{7}$$

where the set Ω_i represents all the pedestrians and obstacles in the neighborhood of the pedestrian i, and the term $S_{i,j}^k$ represents how much the pedestrian i is walking away from j, inside the lattice k. Its value varies in the interval $[0, 1]$, and is calculated by:

$$S_{i,j}^k = \begin{cases} 1, & j \text{ doesn't intersect } k \\ A_{i,j}^k + (1 - A_{i,j}^k) B_{i,j}^k, & \text{otherwise,} \end{cases} \tag{8}$$

where the value of A_{ij}^k represents a percentage of separation between the pedestrian i and the part of the pedestrian (or obstacle) j which has an intersection with the lattice k. This measure is obtained by:

$$A_{i,j}^k = \begin{cases} 0, & \text{se} \quad H_{i,j}^k \leq \eta \\ \frac{H_{i,j}^k - \eta}{\rho - H_{i,j}^k}, & \text{se} \quad \eta < H_{i,j}^k < \rho \\ 1, & \text{se} \quad H_{i,j}^k \geq \rho, \end{cases} \tag{9}$$

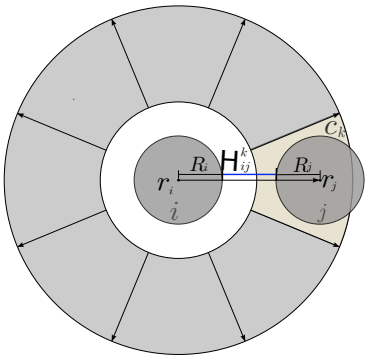

(a) Central point of j is at the lattice c_k.

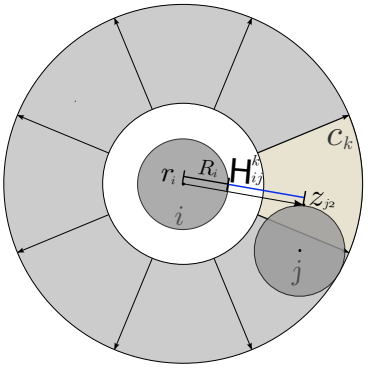

(b) There is an endpoint of j at the lattice c_k.

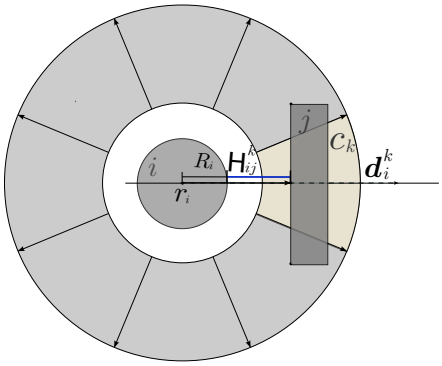

(c) Neither the central point of j nor its endpoints are at c_k.

Fig. 7. Distance $H_{i,j}^k$ used in the calculation of $A_{i,j}^k$ in three possible situations.

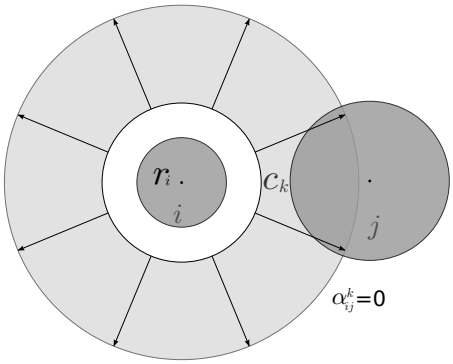

(a) None endpoint of j is inside the region of the lattice c_k ($\alpha_{i,j}^k = 0$).

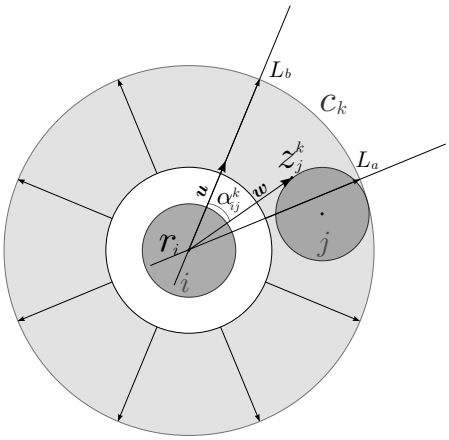

(b) Pedestrian j does not occupy all the lattice c_k.

Fig. 8. Free angular opening of the lattice c_k.

where ρ is related to the radius of the neighborhood of the pedestrian i, and j is a neighbor pedestrian. ρ has the same value of the constant PR. On the other hand, being j a neighbor obstacle, ρ has the same value of the constant OR. Such constants determine the inferior and superior quota, respectively, for the value of $H_{i,j}^k$, which, in turn, represents the part of i inside the lattice c_k, as it is illustrated by Fig. 7. In the Equation 6, the term $B_{i,j}^k$ represents the percentage of θ, which is the angular opening of the lattice c_k that is not occupied by the part of the pedestrian j that lies on the lattice c_k. This term is calculated by:

$$B_{i,j}^k = \frac{\alpha_{i,j}^k}{\theta}, \tag{10}$$

where the term $\alpha_{i,j}^k$ is an angular value in the interval $[0, \theta]$ and represents a free angular opening of the lattice c_k. In the case of non-occurrence of any endpoint of j inside the region of the lattice c_k, $\alpha_{i,j}^k$ must assume a null value, as illustrated in Fig. 8a. This happens when j occupies c_k so that any angular opening is free, as observed in Fig. 8b. Still referring to Equation 6, the term D_i^k represents the strength that makes a pedestrian walk towards its target according to the vector d_i^0

$$D_i^k = D\frac{(cos(\theta_{i,0}) + 1)^2}{4}, \tag{11}$$

where the drift D, of which value is between 0 and 1, represents the TODO:strength drifting in the direction d_i^0 from the pedestrian's current position to exit. $\theta_{i,0}$ is the angle between the unit vector in direction d_i^k and the unit vector in direction d_i^0. The term N is a normalization factor responsible for ensuring that $\sum_d P_i^k = 1$. The term δ_i^k represents the fact that people do not prefer directions where there are others extremely near them, in conditions of low and medium densities. It can assume the value 0 or 1 as follows:

$$\delta_i^k = \begin{cases} 0, & \text{se} \quad Access_i^k = 0 \\ 1, & \text{se} \quad Access_i^k \neq 0. \end{cases} \tag{12}$$

Finally, the term I^k is bigger than 1 when the chosen direction in the previous step is related to the lattice k, otherwise its value is 1. This term represents the preference of a pedestrian for maintaining the chosen direction of its previous movement.

C. New desired direction of motion

The sum of access terms for a pedestrian i sets a rate of occupancy of the space around it. If this sum is above a threshold λ, this indicates that there is space for the pedestrian to go around other pedestrians. Otherwise, the pedestrian will keep the direction of motion similar to the SF model.

Thus, after calculating the weights of each lattice of the grid, if the sum of the factors of access is above the threshold λ, the desired direction e_i of the pedestrian i will be the direction of the lattice that received the greatest weight. Otherwise, the direction will be equal to d_i^0.

IV. Experiments

In this section we present some simulations using the SF model altered with our modifications described above. We conducted experiments to verify that the modified model produces changes in the paths of the pedestrians, while the crowd maintains the ability to reproduce the "Faster-is-slower" effect and the arching underlying the clogging effects.

In all scenarios, people are randomly distributed in space. People are represented as circles whose radii obey a Gaussian distribution with mean $0.6\,m$ and standard deviation $0.1\,m$. We suppose these people are in danger and they attempt to leave the room using only one door.

The parameters used in the simulations, in Equations 2, 3 and 4, are initialized as follows: $\tau = 0.5\,s$, $A = 2 \cdot 10^3\,N$ (Newtons), $B = 0.08\,m$, $K = 1.2 \cdot 10^5 kg/s^2$ and $\kappa = 2.4 \cdot 10^5\,kg/m/s$. The specific input data to our model are: the grid has 8 lattices, the radius of the neighborhood in relation to other pedestrians PR is $0.8\,m$, the radius of the neighborhood in relation to obstacles OR is $4.0\,m$, η is $0.4\,m$, the threshold λ is 1.25, the inertia in the previous direction I^k is 1.2, and the drift D is 1.0.

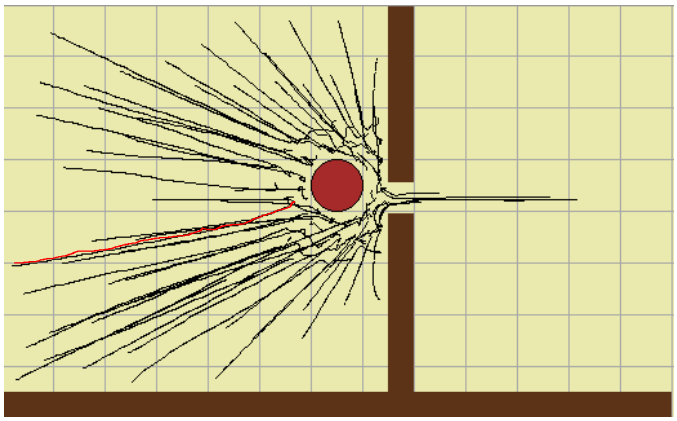

(a) Simulation with the SF model.

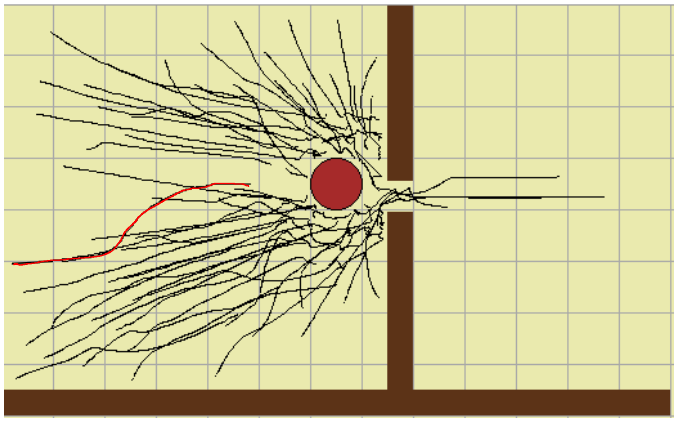

(b) Simulation with the modified model.

Fig. 9. Trajectories of pedestrians in the first experiment.

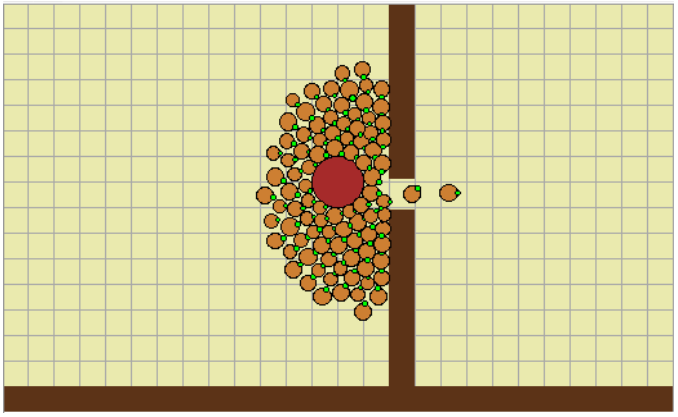

Fig. 10. Screenshot of the first experiment $5.38\,s$ after initialisation.

The trajectories of the pedestrians: The first experiment checks the trajectories of the pedestrians in a scenario of evacuation of a room with a single door. It aims to verify the improvements of the trajectories by comparing the proposed modifications with the previous model [1].

The scenario for starting the simulation is set as follows. In a $15\,m \times 15\,m$ room with a $1.2\,m$ wide door, there is a column near it with a $2\,m$ radius, and there are 60 randomly distributed pedestrians with the same desired velocity $v^0 = 5\,m/s$. The trajectories of the pedestrians resulting from the simulation of this scenario are shown as black lines in Fig. 9, where (a) shows results for the original model, and (b) shows results for the modified model.

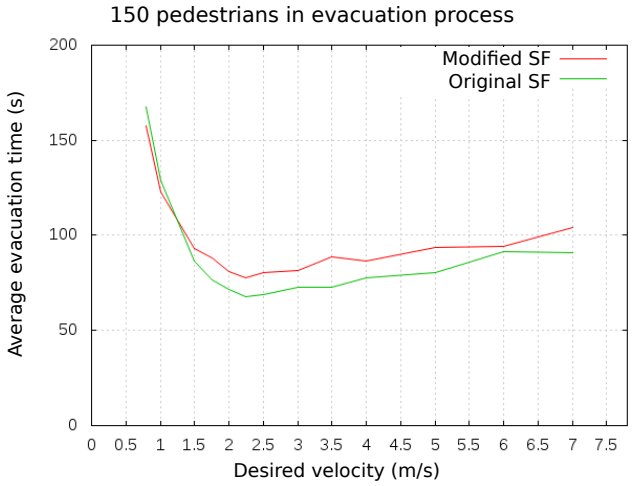

Fig. 11. Evacuation times of the pedestrians for various desired velocities v^0.

Leaving times of pedestrians for various desired velocities: The second experiment checks the average evacuation times for pedestrians in the scenario of a room with a single door against different desired velocities. It aims to verify if the time for all pedestrians to leave the room decreases when growing the desired velocities by a certain value, comparing it with the original model.

The scenario for starting the simulation is set as follows. In a room similar to that described above, but without the column, there are 150 randomly distributed pedestrians with the same desired velocity. Each simulation is set with the following values for the desired velocities v^0: 0.8, 1.0, 1.5, 1.75, 2.0, 2.25, 2.5, 3.0, 3.5, 4.0, 5.0, 6.0, and 7.0. Fig. 11 shows the relation between the average evacuation time and the desired velocity, obtained from simulations with the original and the modified models.

V. Results and Discussion

In this section we present and discuss the obtained results according to the above-mentioned experiments.

In the first experiment we observe that the modified model produces changes in the trajectories of the pedestrians when compared to the trajectories produced by the original one. The trajectories of the original model are similar to straight lines, since pedestrians do not deviate from the column neither from the other pedestrians, even when there is the possibility to circumvent them.

To illustrate this situation, in Fig. 9, the red line represents the trajectory of a pedestrian. The line produced by the original model is straight (Fig. 9a). On the other hand, the

line produced by the modified model is curved (Fig. 9b). This occurred by the changes applied to the pedestrian's desired direction. The same behavior occurs for the other trajectories.

Additionally, one can observe the appearance of arching near the exit, even for a simulation with the modified model, according to Fig. 10 (pedestrians are represented by orange circles). This shows that the modified model is also able to reproduce the arching underlying the clogging effect.

In the second experiment, we observe the Faster-is-slower effect. For values of v^0 lower than $2.25\,m/s$, the time for 150 pedestrians to leave the room decreases with growing v^0, in both models (Fig. 11). On the other hand, for $v^0 > 2.25\,m/s$ the time for them to leave the room increases. This is related to clogging near the exit; the pedestrians trying to move faster cause a smaller average speed of leaving and, consequently, slower evacuation.

Although the evacuation times, for the models, have been slightly different, the curves exhibit the same behavior, i.e. they have the same inflection point ($v^0 = 2.25\,m/s$). This shows that the modified model maintained the expected Faster-is-slower effects.

VI. Conclusion

Helbing and Molnar's SF model [1] as well as our proposed extension to their work have a great potential to simulate dynamic aspects of the evacuation process.

We present a modification of the force of desire in order to let pedestrians change their desired directions of movement voluntarily, based on their perceptions of other pedestrians and obstacles in their neighborhood. For that, we proposed the use of a mobile grid inspired by the lattice-gas model [2].

Our results showed that the modified model improves the trajectories of the pedestrians, while it maintains the ability to reproduce the "Faster-is-slower" effect and the arching underlying the clogging effects.

Nevertheless, our model, as well as the original one, does not deal with occlusions explicitly, i.e. two pedestrians could occupy the same space, if the parameter values were indiscriminately set.

The method was not designed for real time applications. Our first prototype generates text files containing descriptions of scenes, which are later used by a program developed by us to generate the visualization of the simulation. The time spent to create each scene increases with the number of interactions that occur among pedestrians. In future works, we intend to make quantitative assessments of the time spent to produce the scenes and check their use in real-time applications.

Also in future works, we intend to submit the modified model to scenarios with counterflow. Additionally, we intend to investigate if our model is able to simulate the effects of stop-and-go waves, and the phenomenon called crowd turbulence, observed in real crowds in [10].

Acknowledgment

We would like to thank CNPq for the financial support. We also express our gratitude to Dirk Helbing, Illés Farkas and Tamás Vicsek for kindly providing us with their source code.

References

[1] D. Helbing, I. Farkas, and T. Vicsek, "Simulating dynamical features of escape panic," *Nature*, vol. 407, no. 6803, pp. 487–490, September 2000. [Online]. Available: http://dx.doi.org/10.1038/35035023

[2] R. Y. Guo and H. J. Huang, "A mobile lattice gas model for simulating pedestrian evacuation," *Physica A: Statistical Mechanics and its Applications*, vol. 387, no. 2-3, pp. 580 – 586, 2008. [Online]. Available: http://www.sciencedirect.com/science/article/B6TVG-4PTW4PD-3/2/5e4637d892fd3df83ea4354f87048c82

[3] A. Varas, M. D. Cornejo, D. Mainemer, B. Toledo, J. Rogan, V. Munoz, and J. Valdivia, "Cellular automaton model for evacuation process with obstacles," *Physica A: Statistical Mechanics and its Applications*, vol. 382, no. 2, pp. 631 – 642, 2007. [Online]. Available: http://www.sciencedirect.com/science/article/B6TVG-4NJ0THF-3/2/bfa1d5b12c6a59d82be0a77d411f11c2

[4] G. J. Perez, G. Tapang, M. Lim, and C. Saloma, "Streaming, disruptive interference and power-law behavior in the exit dynamics of confined pedestrians," *Physica A: Statistical Mechanics and its Applications*, vol. 312, no. 3-4, pp. 609 – 618, 2002. [Online]. Available: http://www.sciencedirect.com/science/article/B6TVG-464P5B9-3/2/3fd73fc24e660346619b82fb66269a67

[5] M. Muramatsu, T. Irie, and T. Nagatani, "Jamming transition in pedestrian counter flow," *Physica A: Statistical and Theoretical Physics*, vol. 267, no. 3-4, pp. 487 – 498, 1999. [Online]. Available: http://www.sciencedirect.com/science/article/B6TVG-3WN6W3W-H/2/439ff55f3e6f8ffa376d0e07f2cee5a9

[6] Y. Tajima and T. Nagatani, "Scaling behavior of crowd flow outside a hall," *Physica A: Statistical Mechanics and its Applications*, vol. 292, no. 1-4, pp. 545 – 554, 2001. [Online]. Available: http://www.sciencedirect.com/science/article/B6TVG-42DP3B7-1F/2/958767cfdb062ad73d32e09f9bbd0da0

[7] R. L. Hughes, "A continuum theory for the flow of pedestrians," *Transportation Research Part B: Methodological*, vol. 36, no. 6, pp. 507 – 535, 2002. [Online]. Available: http://www.sciencedirect.com/science/article/B6V99-43SW91M-1/2/7b10c7a5a89ce902487152bcd96912f2

[8] L. Huang, S. C. Wong, M. Zhang, C. Shu, and W. H. K. Lam, "Revisiting Hughes' dynamic continuum model for pedestrian flow and the development of an efficient solution algorithm," *Transportation Research Part B: Methodological*, vol. 43, no. 1, pp. 127 – 141, 2009. [Online]. Available: http://www.sciencedirect.com/science/article/B6V99-4T3TPRB-2/2/deb9256e4c5babb942ec027517b0de3c

[9] A. Treuille, S. Cooper, and Z. Popović, "Continuum crowds," in *SIGGRAPH '06: ACM SIGGRAPH 2006 Papers*. New York, NY, USA: ACM, 2006, pp. 1160–1168.

[10] D. Helbing, A. Johansson, and H. Z. Al-Abideen, "The dynamics of crowd disasters: An empirical study," *Physical Review E (Statistical, Nonlinear, and Soft Matter Physics)*, vol. 75, no. 4, Feb 2007. [Online]. Available: http://dx.doi.org/10.1103/PhysRevE.75.046109